

Title

15/U711 - An innovative self-centring slip-friction connection system for seismic damage avoidance design of hybrid timber-steel moment resisting frames

Principal Researchers

*Dr Armin Valadbeigi and Prof Pierre Quenneville
The University of Auckland*

Other Research team Members

*Dr Pouyan Zarnani, AUT
Assoc-Prof Charles Clifton, UoA*

Key words

Seismic, resilience, ductility, low-damage, friction, re-centring, connection

Summary

The slip friction devices have been studied and tested by several researchers. It has been proved that this type of damper demonstrates a straightforward and effective way of damping energy. The main disadvantage of conventional friction devices is a lack of self-centring characteristic, which in earthquake loadings can lead to a permanent drift of structures. Recently, an innovative Resilient Slip Friction Joint (RSFJ) has been developed at the University of Auckland to address this shortcoming. This study aims to investigate the potential application of the newly introduced resilient slip friction connection for hybrid steel-timber structures. This concept is used to provide both energy dissipation and a self-centring feature for structures. The hybrid systems have grown prevalent as a method of multi-storey construction. As for the steel-timber building, the high ductility of steel can improve the post yielding behaviour of timber structures and timber members can enhance fire resistance of the structures. Initially, the conventional slip friction devices have been analytically mounted on a 10-storey timber structure to determine the influence of sliding force variability on the response of the structure. A nonlinear time history analysis was conducted to determine the optimum sliding force for friction connections and, more importantly, to investigate their ability in restoring the structure to its original position.

In the next step, a new system (RSFJ) was introduced. The idea of the RSFJ was determined and tested experimentally to show the ability of the connection to provide self-centring characteristic. Therefore, an RSFJ with 120 kN capacity was designed and manufactured to be studied experimentally. The equations presented to correlate a sliding force with a coefficient of friction and to predict the hysteresis curve of the connection. All the equations were validated through experiments.

This research provides the detailed information of the RSFJ to be used in the hybrid steel-timber or timber structures. Since the behaviour of the joint is complicated and could not be easily captured through static and geometry of the joint, a very detailed and intricate model was required to investigate every aspect of

the joint. The finite element analysis (FEA) was carried out using ABAQUS software as a method to observe the distribution of stress in the different parts of the connection. Thus, the RSFJ was modelled and analysed using an FEA to investigate the parameters which are difficult to measure during the experiments. The FEA used to design the first RSFJ with 1000 kN capacity and the RSFJ used for a full-scale test.

A full-scale connection test was conducted to investigate the self-centring characteristic and to provide practical details for the assembly purpose. Afterwards, a full-scale column test was carried out to demonstrate the behaviour of the RSFJ in a full-scale experiment. The results were employed for the construction of the new Nelson Airport Terminal. Finally, the ductility of a 10-storey hybrid building equipped with RSFJ was investigated to establish a procedure for computing the ductility factor.

Introduction

Lateral load resisting systems with self-centring (SC) ability are relatively new earthquake-resistant structural systems. They are designed to not change the stiffness and strength of the structural system while limiting the drift value and the members damage under a seismic excitation.

In contrast to conventional structural systems, SC systems have targeted connections that decompress and open at a specific level of earthquake loading, starting rigid-body rocking within the system. The post-tensioning (PT) bars are quite common in the self-centring system as they supply the restoring force for the connections to bring the structure back to the initial position. From another point of view, the rocking behaviour of the system provides energy dissipation which could lead to the peak seismic response reduction.

The SC concept was first developed for concrete structures [1,2]. As it is shown in Figure 1, Kurama et al. proposed a design procedure for unbounded post-tensioned precast concrete walls. The main feature was to limit the earthquake-induced damage that occurs in concrete shear walls [2]. After that, seismic-resistant steel braced frame systems were developed based on the mentioned concept [3,4].

Priestley et al. experimented the unbounded prestressed and post-tensioned concrete frames. A scaled five-storey precast structure was studied under seismic loading [4]. The results proved that the building had low structural damage and low residual drift. SC seismic resistant steel moment-resisting frame systems were developed based on the same concept [5,6,7,8]. An example of such a system is shown in Figure 2.

Furthermore, the application of SC systems has been expanded to rocking concentrically braced frame systems which can accommodate large drift while having minimal residual drift compared to the conventional CBF systems [3,4]. This system is schematically presented in Figure 3.

The system is intended to decompress at the base when the lateral load reaches a specific level. Rocking on the base would dissipate the input energy. The system requires another set of columns to separate the lateral load carrying frame from the gravity frame.

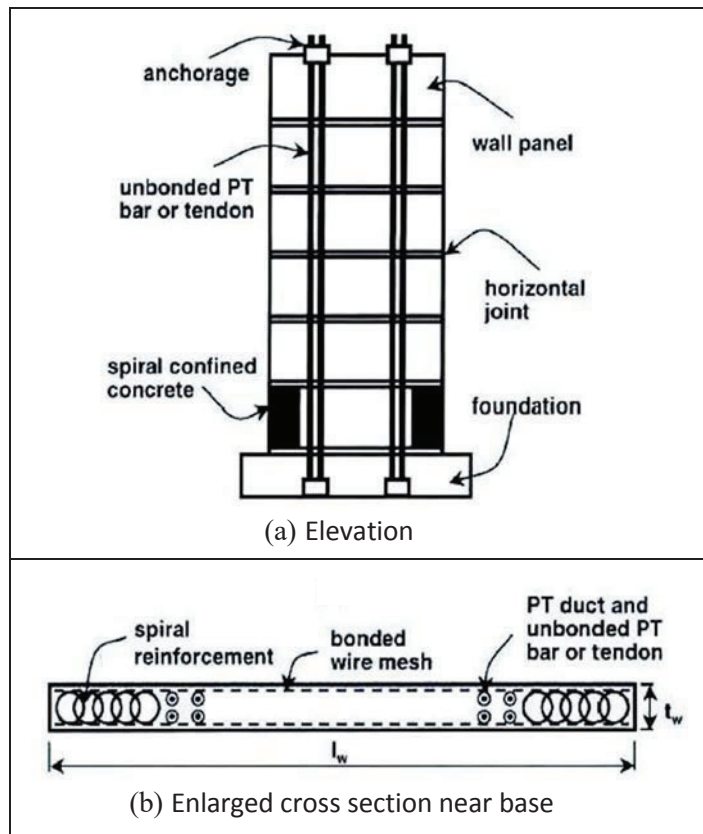


Figure 1: Unbounded post-tensioned precast wall [1]

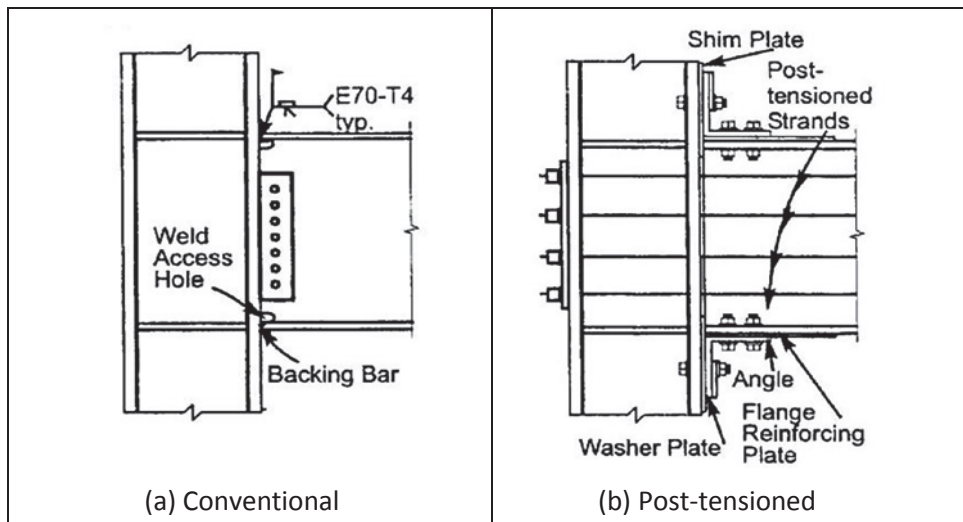


Figure 2: Moment resisting connection [5]

This allows the rocking behaviour while avoiding the slabs damage. The friction between the lateral load resisting frame and the gravity frame is used as an energy dissipation mechanism

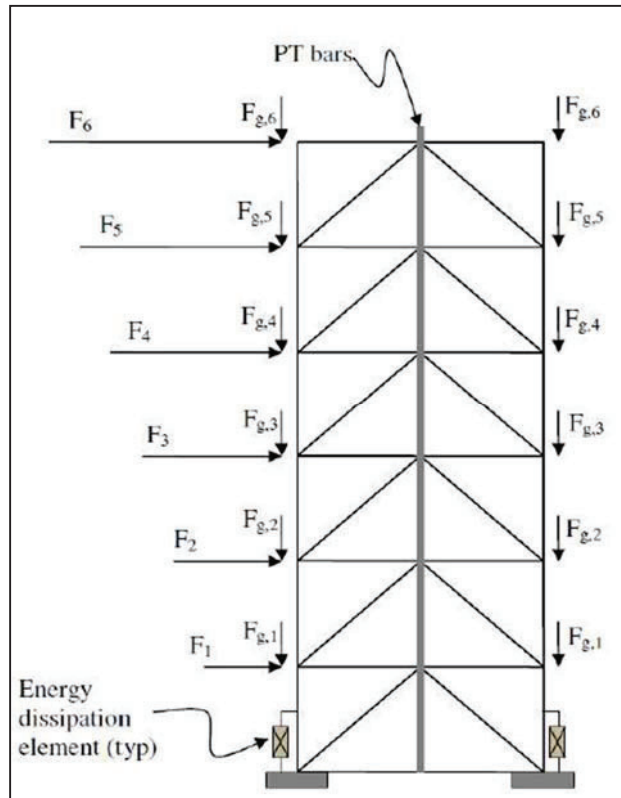


Figure 3: Schematic of an SC-CBF system [9]

Danner and Clifton investigated the possibility of using PT bars incorporating ring springs in the beam-column connection, emulating the PRESSS system used in concrete structures [10,11]. The ring spring option is shown in Figure 4. The connection shows gap-opening under considerable storey drift which causes significant damage to the overlying slab. Therefore, they are considered impractical for beam-column connections, and it is suggested to use this system at the column bases.

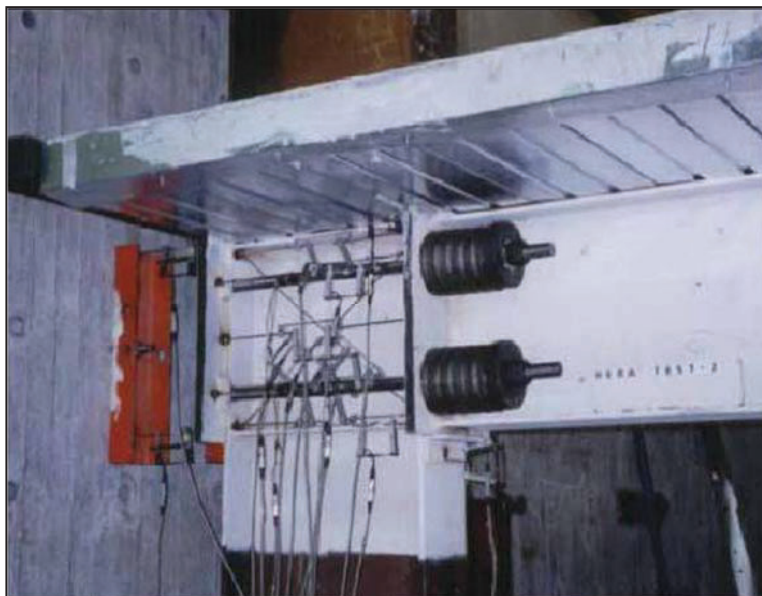


Figure 4: Ring spring joint [12]

floor partially restrains the expansion. Garlock and Li proposed using collector beams to transfer the

force as a method to mitigate these effects [13]. King, and Chou and Chen suggested providing an intermittent slab or connecting the slab to a solid span and permitting sliding in the other spans to allow deformation. These systems were tested showing their effectiveness in isolating the floor slab during inelastic rotation of the joints. However, none of these methods can be simply employed on full-scale frames without introducing secondary damage. Therefore, there is a need for a self-centred sliding joint which is free of the problems mentioned above and can be easily adopted by the industry [14,15].

A hybrid building employs at least two materials. Technically all timber buildings are hybrid systems as the connections are almost always made of steel. The hybridisation can be broken down into three types: component hybridisation, system hybridisation, and building hybridisation. Hybridisation can also be happened in the component level which involves using two materials for a member. One typical example of component level hybridisation for a timber-steel hybrid is a flitch beam, composed of steel plates sandwiched between pieces of timber. In this case, the strength considerably higher compared to the timber beam and another advantage is that the timber provides lateral restraint for the steel to prevent the torsional buckling. The steel and wood are connected using bolts spread over the length of the beam to transfer shear. This connection is the crucial part of the design to ensure that appropriate distribution of forces occurs without splitting in the wood.

System-level hybridisation entails the use of multiple material types within a structural system. A typical example of a hybrid system is steel and wood trusses. Building level hybridisation is the combination of building systems of different materials. One example of this is a vertically mixed system. Vertically mixed systems have been completed around the world, with one timber vertically mixed system in Australia becoming the tallest timber residential building in the world. The lower floors, which support more load and often have a higher storey height, are constructed entirely from concrete or steel framing; the storeys above are then timber-framed. The result is a significantly reduced the weight of the building, the size of the foundations as well as the requirements for the lower storeys design. The stronger material type at the lower floors prevents the requirement for larger timber sizes at these levels.

The hybridisation of a building using steel and timber is not prevalent as steel and concrete hybridisation but there are some buildings that are studied in this regard. One such case study is reviewed here, the Quebec hybrid office building. This six storey hybrid building has been constructed in Quebec, Canada. The system is a heavy timber framing with concrete shear walls as shown in Figure 5.

The wood framed solution is significantly lighter than a concrete column and slab. This will reduce the total weight of the building, which will reduce the foundations and seismic design load. It can result in a building being governed by wind design

Friction connections

The slotted bolted connection (SBC) is a type of friction connection which provides ductility and energy dissipation.



Figure 5: Six storey wood and concrete hybrid building structure [16]

The hysteresis behaviour of the SBC is a non-linear curve where the slip initiates at a predetermined force depending on the friction coefficient and the clamping force. The previous studies on the friction dampers showed that the slippage in these connections leads to considerable loss in the prestressing force of the bolts [17]. Further research was carried out on the sliding behaviour between mild steel surfaces and brass surfaces. The tests were conducted on SBCs with symmetric sliding details. The SBC (Fig. 6) has the main plate sandwiched by brass shims and also two steel plates. All the components are bolted together where only the main plate has slotted holes to allow the sliding. It was shown that this combination has a repeatable hysteresis behaviour. [18,19].

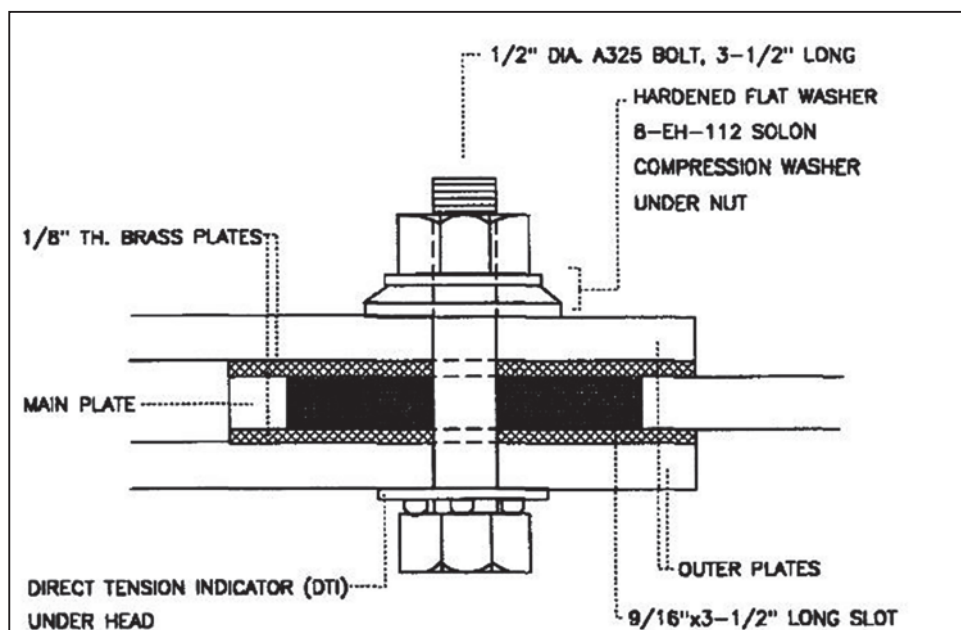


Figure 6: Details of slotted bolted connection [19]

Yang and Popov then employed the SBC and presented a moment connection by having two SBCs at the

top and the bottom of the beam. The joint configuration is shown in Figure 7. However, the overall cost of the system is quite high and the construction and fabrication has some difficulties [20].

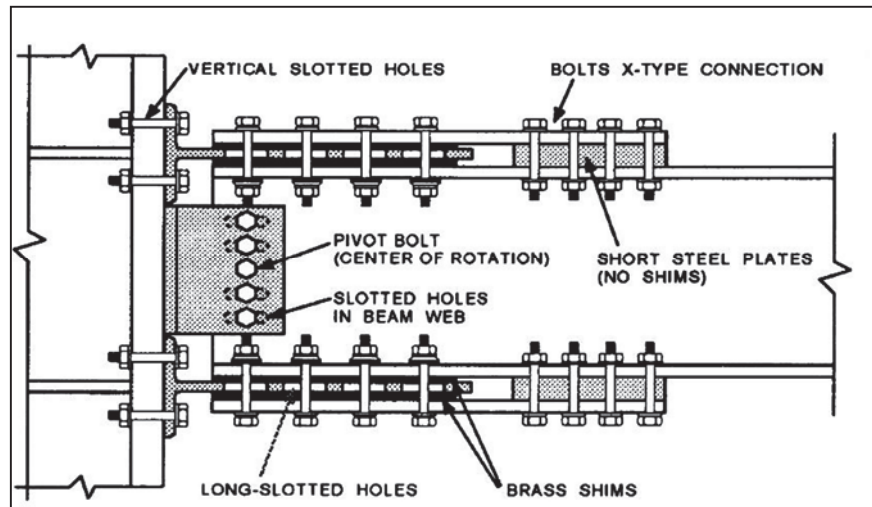


Figure 7: Rotational slotted bolted connections [20]

Furthermore, the behaviour of the SBC in the top flange is influenced by the presence of a suspended slab. As such, this concept was adapted to the development of the Sliding Hinge Joint by Clifton, which utilised the Asymmetric Friction Connection (AFC), and involved sliding only in the bottom flange [12]. The Sliding Hinge Joint (SHJ) which is considered as a low damage connection comparing to the traditional connection was introduced by the New Zealand Heavy Engineering Research Association (HERA) and the University of Auckland [12]. The beam and the column are connected from the top flange plate, bottom flange plate and web plate. All the plates are bolted to the beam and welded to the column. Their description and design roles are as follows:

1. The top flange plate provides a robust connection that pins the top corner of the beam, which provides a point of rotation under inelastic rotation and limits gap opening.
2. The bottom flange bolt group consist of Asymmetric Friction Connections (AFCs). When the AFC slides, it dissipates energy through the friction between the plates.
3. The connection has two rows of bolts in the web. The top web bolt group is designed to resist joint shear while the bottom web AFC slides during inelastic joint rotation.

Before the sliding occurs, the SHJ acts as a rigid connection but when sliding initiates the beam rotates about the top flange plate where it is connected to the column and part of the energy is dissipated through friction. The AFCs decouple joint strength and stiffness, confines yielding to the bolts, and also the inelastic demand in beam and the column would be limited. The top flange plate was shown experimentally not to undergo net elongation during inelastic rotation, which limits beam growth. Testing also showed that when the rotation point is at the top flange, it isolates the floor slab which reduces the damage to the slab. The slab may be subject to minor cracking which is easily repairable [21].

The AFC is a type of slotted bolted connection with a different configuration from the symmetric

sliding conditions tested by Grigorian and Popov [18]. The details and the hysteresis curve of the AFC is demonstrated in Figure 8(a). The plates are clamped together with high strength bolts. The bolts are installed following the turn-of-nut method in accordance with NZS 3404. [22]. When the force exceeds the frictional resistance of the surface, the sliding starts in the first interface (point B). With increasing the force, sliding starts in the second interface (point C). The force that requires to initiate the second sliding is about twice the force for the first sliding. At this state, the bolts are under double curvature. Another sliding occurs in the first interface as it builds up (point D) which follows with another sliding in the second interface (point E) since the double curvature in the bolts go into the opposite direction. This provides pinching in the hysteresis curve. The connection is designed to be rigid under the serviceability level earthquake and slide under the design level earthquake.

The travel length provided for the slotted holes allows up to 35 milliradians (mrad) rotation, which is higher than the expected rotation under the DLE load. This is calculated based on the inter-storey drift limit with a safety factor of 1.4 under the maximum credible earthquake (MCE). The SHJ would maintain integrity but undergo controlled damage as the bolts might want to go beyond the slotted holes. This is where there is a possibility of ductile failure since yielding is probable in the bottom flange. This ductile failure mechanism where the joint integrity was maintained was shown experimentally by Clifton, where the SHJ was still able to deliver the design moment capacity at 120 mrad of rotation. Following the MCE loading, components in the SHJ such as the bottom flange plate and web plates might require remedial or replacement [12].

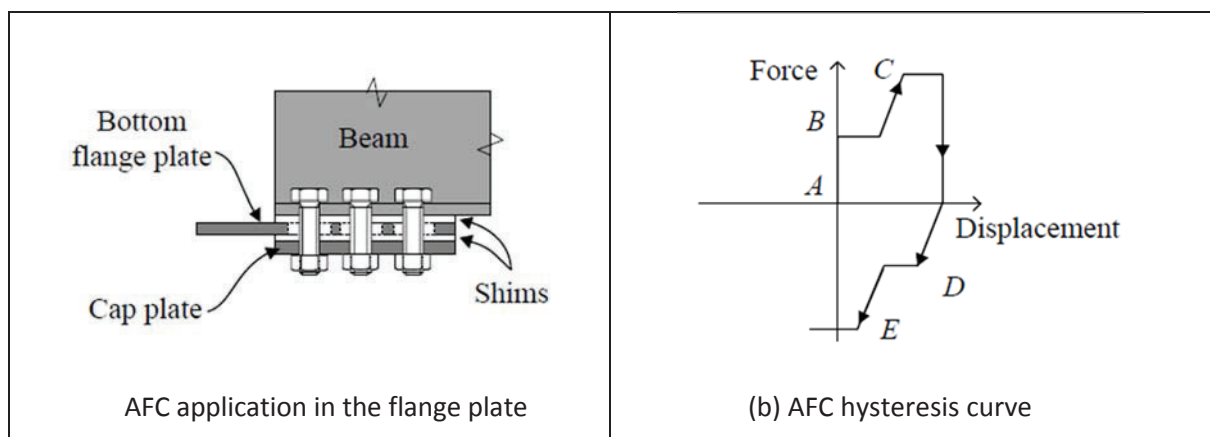


Figure 8: AFC hysteresis behaviour [21]

Clifton conducted four tests on two full-scale SHJ subassemblies, each consisting of a 610UB101 external column and a 530UB82 beam. The tests were at quasi-static rates of loading. The first two tests (on the first subassembly) showed the viability of the rotational concept of the joint about the top flange plate and the AFC sliding behaviour. However, the joint displayed significant degradation in strength due to insufficient clearance between the column and the beam. The moment-rotational response of Test 3 by Clifton is shown in Figure 9 [12]. The behaviour of the SHJ was further tested by MacRae et al. [21].

The floor slab gets isolated when the point of rotation is about the top flange plate and it limits the effects of beam growth and frame expansion. As such, the SHJ is not susceptible to frame expansion and additional

demands on the columns and floor slab as the PT systems previously described. However, the top and bottom flange plates are also subject to inelastic demands during joint rotation.

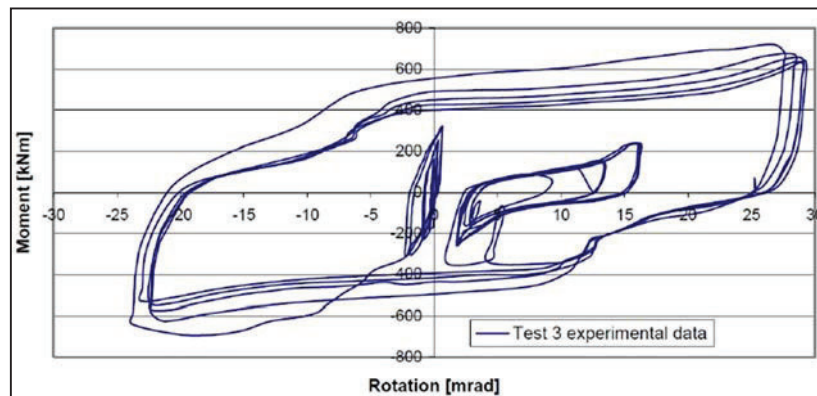


Figure 9: Experimental moment-rotational behaviour of Test 3 from Clifton [12]

Advantages and limitations

As the SHJ inelastic demand is confined to the connection as opposed to typical elastoplastic beam hinging.

The advantages of the SHJ over the conventional beam-column connections are as follows:

- a. Moment frame strength and stiffness is decoupled, which allows the use of large beam sizes to control frame lateral stiffness and drifts, without imposing high over-strength demands on the columns.*
- b. Inelastic demand is confined to the bolts in the AFC, that can be replaced after a ground motion. Other joint components are subject to negligible inelastic demands and do not require replacement.*
- c. Lower cost due to reductions in column section sizes.*

The two main limitations of the SHJ are as follows:

- a. While time-history analyses of 10 storey frames showed that the SHJ has a tendency to dynamically re-centre due to the "pinched" hysteretic curve, the studies showed that frames with the SHJ could have residual drifts under a major earthquake. This can have substantial impact on the overall repair cost of the building.*
- b. The main goal of the SHJ is to re-gain its rigidity after the DLE load which the research experimentally and analytically showed that this was not achieved, and the bolts have to be replaced [2].*

This research aims to enhance the concept of SHJs by introducing the RSFJ to add a self-centring feature to the connection.

Objectives

Steel-timber hybrid systems can compete with concrete and steel structures; however, in current building codes and material design standards, there is a lack of guidelines on the seismic design of hybrid systems. Therefore, experimental and analytical studies are much required to evaluate the behaviour of the system, identify the possible challenges, establish a design guideline, and propose a practical installation method. Friction damped hybrid steel-timber frames with RSFJ having self-centring feature is being developed to provide considerable drift capacity while and reduce the structural damage and the residual drift. The main goal of this research is to explore the possibility of RSFJs' application in the structural system. To achieve this goal and develop connection details to ensure the efficiency of RSFJs in structures this research covered the following objectives:

- a. Investigate the behaviour of conventional slip friction joints and demonstrate their performance in various structures;
- b. Specify a range for the sliding force of conventional slip friction joints;
- c. Design and test the first RSFJ sample (120 kN capacity) to verify the theoretical formulas;
- d. Test different RSFJs as well as different grease types to come up with the most smooth and repeatable joint behaviour;
- e. Develop finite element models of the RSFJ to help design the first 1000 kN capacity joint and investigate the behaviour of the middle and cap plates.
- f. Conduct in-plane testing of a full-scale RSFJ to assess the response of the connection under static loading.
- g. Test the proposed RSFJ to determine the damping ratio of the joint.
- h. Test a full-scale moment resisting steel column/LVL beam equipped with the RSFJs to evaluate the behaviour of a real size system.
- i. Investigate a conceptual ten-storey structure as a subject of this study and determine the ductility factor for such a building equipped with RSFJs.
- j. Conduct time history analyses of the steel-timber hybrid building with the RSJs and compare the results with a building having conventional connection.

Results

Joint configuration

The RSFJ configuration is presented in Figure 10, including each of the joint components. The joint consists of two cap plates and two middle plates. All the parts are joined by bolts while the disc springs are situated at the top and the bottom of the joint. The plates have triangular grooves to provide interlocking of the plates. The middle plates are provided with elongated holes to allow the horizontal movement. Disc springs answer the need for vertical movements of the cap plates when the gap is going to exist.



Figure 10: Resilient slip friction joint

An essential factor to avoid galling effects, scratches and ensure a long service life is sufficient lubrication of the plates. All the contact surfaces should be lubricated with special grease before assembling the RSFJ. To enhance the hysteresis behaviour of the RSFJ and decrease the residual drift to a minimum, a grease was applied to the plates to solve the galling effect problem and ensure a complete self-centred connection. The tests have been conducted with various sliding force to determine the friction coefficient in the new system (Figure 11).

The first test conducted with a 20 kN sliding force, the second one performed with a 30 kN sliding force and the last test carried out with a 40 kN sliding force to study the influence of sliding force on damping ratio of the joint. SAP 2000 [23] was used to model RSF joints in a building. The hysteresis behaviour of the RSFJ should be modelled using the link element in SAP 2000. Among different available link elements, damper-friction spring has been chosen to reflect the behaviour of the joint as it has been defined specifically for the flag-shaped hysteresis curves.



Figure 11: The RSF joint lubricated with grease 1000 kN joint

The RSFJ components are presented in Figure 12. The two one-sided grooved cap plates and two two-sided grooved middle plates are bolted together, in which the bolts are positioned in the middle of the slotted holes of the middle plates. The disc springs are placed on the cap plates to provide room for the upward and downward movement of the cap plates when the horizontal force exceeds the friction force of the plates. The amount of sliding force depends on the prestressing force of the bolts, the angle of the grooves, and the friction coefficient between the plates.



Figure 12: 1000 kN RSFJ

The cap and middle plates are made from hardened and tempered IC 4130 steel with a yield strength of 655 MPa, and a tensile strength of 795 MPa, a 14% elongation and a 30% reduction in area. The experimental test setup is illustrated in Figure 13. The equipment involved in the experiment includes an MTS actuator, a data logger system and a computer. The test setup was assembled on the strong floor of the Auckland University's Test Hall. The end of the actuator was fixed to the strong floor with four prestressed anchors and the other side of the actuator was connected to the attachment.

The attachment itself was also linked to the end plate of the RSFJ. As shown in Figure 13, the portal gauges were installed between the two middle plates of the RSFJ to measure the expansion of the joint. An LVDT and a laser were placed to monitor the vertical movement of the cap plates and to ensure that the connection is behaving symmetrically. Another LVDT was also installed on the end bracket to measure any possible sliding that could influence the test result. The time histories of both displacement and force were recorded by the data logger, which was set up on a 10 per second sampling rate. Figure 13b shows a close-up of the instrumentation and the RSFJ.

The sample was tested cyclically through the end bracket displacement in accordance with the AISC 2005 loading regime. The cyclic loading protocol is in the format of inter-storey drift angle ϑ . The protocol starts with 6 cycles of 3.2 mm ($\vartheta=0.00375rad$) followed by 6 cycles of 4.3 mm ($\vartheta=0.005rad$), 6 cycles of 6.45 mm ($\vartheta=0.0075rad$), 4 cycles of 8.6 mm ($\vartheta=0.01rad$), 2 cycles of 12.9 mm ($\vartheta=0.015rad$), 2 cycles of 17.2 mm ($\vartheta=0.02rad$) and 2 cycles of 20 mm ($\vartheta=0.023rad$). The loading protocol goes to maximum drift of 2.3% since this was the designed criterion. The force-displacement curve of the RSFJ specimen is presented in Figure 14. Initial stiffness (K_0) of the connection is 900 kN/mm, which could be considered a fully restrained connection.



a. Test-setup view



b. Instrumentation

Figure 13: Experimental setup of the RSFJ testing

The connection showed a very consistent and repeatable hysteresis curve while it presented a fully self-centring hysteresis curve in all the cycles with displacement returning to zero in every loop. Therefore, there is not any yielding in the specimen. The repeatable hysteresis behaviour stands for a fact that no major wearing or deep scratches occurred during the test. Meanwhile, the existing discrepancies between FE and the experimental results regarding the unloading stiffness can stem from a couple of reasons including the small scratches on the surface of the plates, which were observed after disassembling the connection, and the uneven surface of the plates in the experiment. The second stiffness (k_1) of the connection is about 30 kN/mm, which is 1/30th of the initial stiffness. The ultimate unloading force is 405 kN which is in good agreement with the analytical data. Additionally, the result confirmed that the residual force is 120 kN. In the compression stage of the test, as predicted, no buckling or yielding was observed under the compression force of 970 kN.

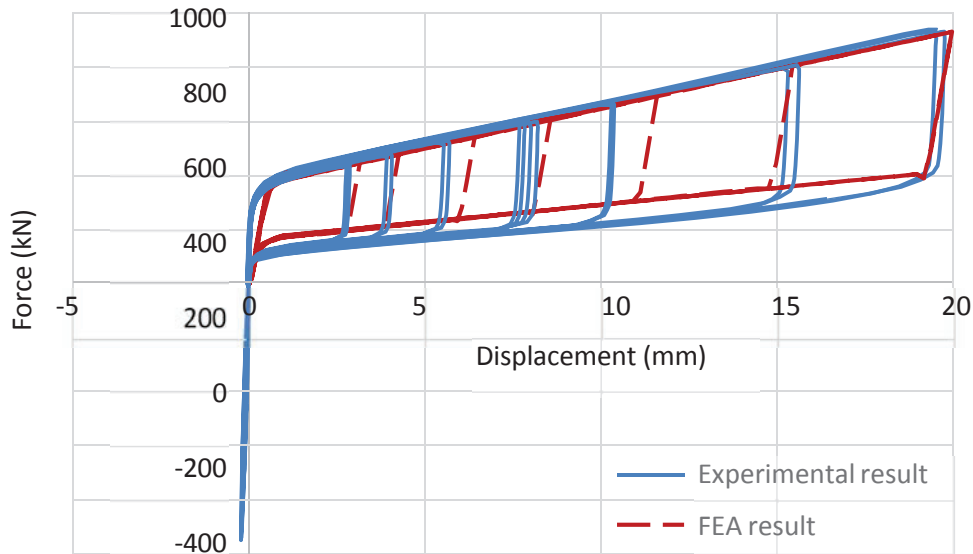


Figure 14: Load-displacement curve

Due to symmetry, only one-fourth of the whole RSFJ model was modelled for the finite-element analysis (Fig. 15). The symmetrical boundary conditions were applied to the cutting planes. Since the RSFJ is symmetrical about the vertical and the horizontal planes, the symmetry conditions were applied along these axes. The connection was designed to remain elastic and behave linearly under the loading protocol. As it is not in the scope of the FEA to investigate the performance of the pin, therefore, it was only modelled to include the influence of the pin deformation in the results. The FE model was employed to obtain the force-displacement response, the initial stiffness and the damping ratio, which was carried out by the following two-stage loading scheme:

- a. The preloading force of the bolts was applied in the first step to prestress the connection. Therefore, all the six bolts were loaded to 60 kN in 10 steps simultaneously.
- b. Applying the displacement by following the loading regime.

A geometric non-linear analysis was carried out to obtain the force-displacement response of the RSFJ. The elastic slip factor of 0.01 was considered for the model. The analysis was conducted using Newton-Raphson equation solver with automatic stepping and the contact algorithm static kinetic exponential decay function.

The solid element C3D8R was employed for the components of the RSFJ. This linear brick element is a general purpose element with decrease integration point. During the analysis procedure, the references points, which were considered in the middle of the cross-sectional areas of the pin, were simultaneously pulled and pushed horizontally using the displacement control loading. A series of mesh study was carried out to evaluate the sensitivity of the results to the different mesh sizes and reach the reasonable mesh size for conducting the FEA. The analyses were conducted under 7 different mesh sizes including, 15 mm, 5 mm, 3 mm, 2 mm, 1.5 mm, 1 mm, and 0.5 mm as for the maximum meshing size in the model. The

assessing criterion for all the analyses was the sliding force of the connection; as a result, the sliding force versus the meshing size where monitored to evaluate and finalise the mesh size. The FE hysteresis curve is backing up the experimental test result. In regards to the experimental test of the RSFJ, the sliding occurs at the force of 400 kN. In the FE simulation, the static solver was employed to carry out the analysis. The sliding force and the second stiffness of the hysteresis behaviour were compared with the experimental results as they are shown in Figure 14. It was observed that the model can precisely simulate the flag-shaped hysteresis curve of the connection.

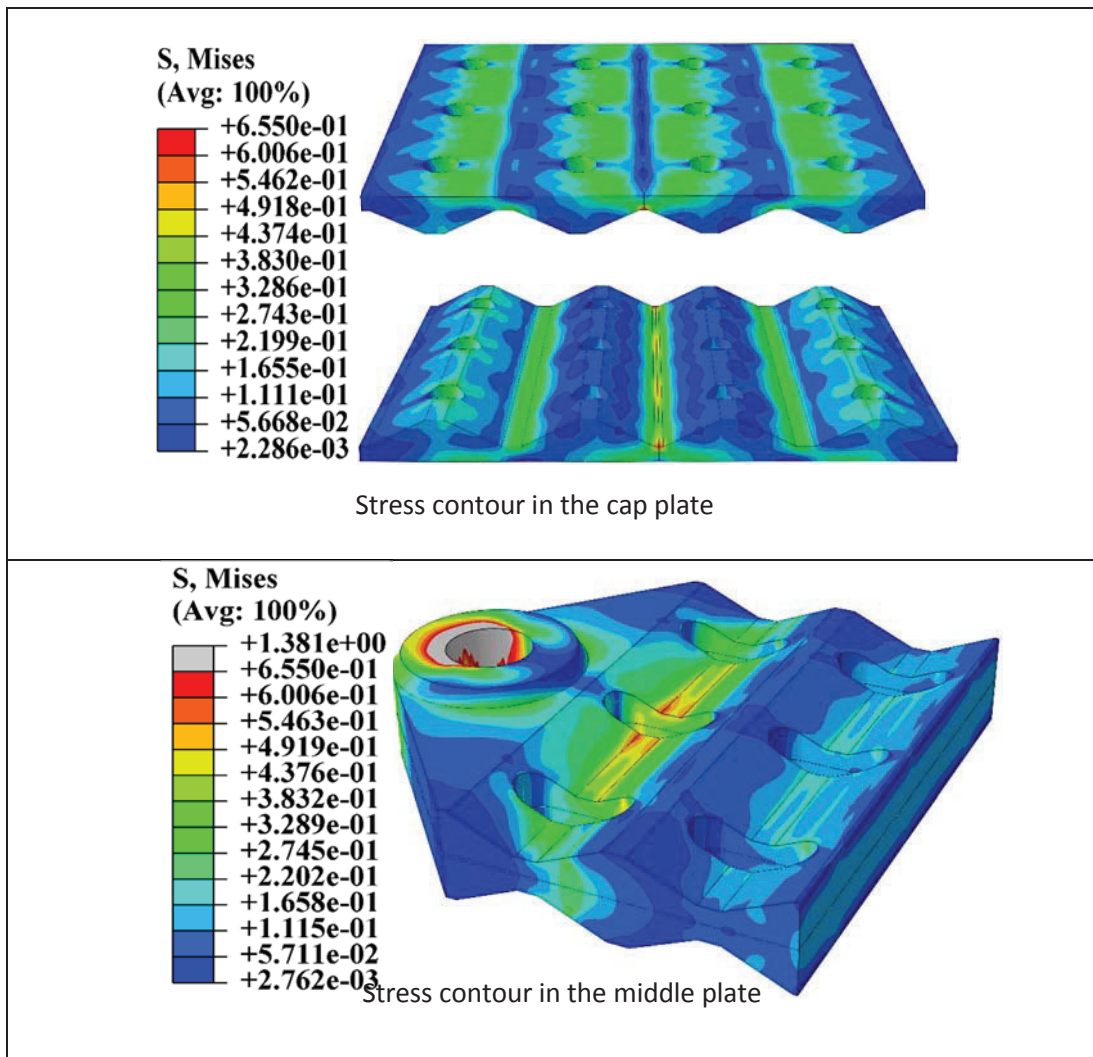


Figure 15: Stress distribution in the RSFJ parts

Consequently, the model can be adopted to predict the maximum stress in the connection. The FEM confirmed the self-centring feature of the system, as the residual drift equals to zero. The maximum stress is below the capacity of the plates except for small areas around the pinhole where we have singularities in the model. The stress singularities arise under different circumstances including the area under the point load, sharp edge locations of the in-contact parts as well as the restraining points. Stress singularities are typical issue in FEA, so those points are not considered for the assessment. Therefore, a specific distance away from these points could be considered for the evaluation. In general, there is turbulence in

the distribution of stress in the elements close to the holes and the boundary condition points. Further from this intensive tension, stress field will get more balanced; these regions are the exact places to be considered for any evaluation objectives.

Investigating the behaviour of the RSFJ is very crucial, since comprehending the behaviour of the RSFJ is a complicated matter. Hence, the finite element analysis is an efficient approach to validate experimental studies. However, finite element modelling of the RSFJ is demanding due to the existence of contact surfaces in the model where this situation affects discontinuities in the stiffnesses of the model. Experimental investigation and the finite element analysis of the RSFJ with 1000 kN capacity corroborated the feasibility of the self-centring feature and demonstrated a repeatable flag-shaped hysteresis curve. The application of the RSFJ as a substitute for the traditional connection enhances the performance of the connection in terms of damage avoidance and energy dissipation capacity. The experimental study proved that the designed connection was able to open up to 20 mm and resist around 1000 kN in both tension and compression without any damage. The connection performed well under different cycles and showed a stable behaviour, which supports the repeatability of the connection. The unwavering force-displacement relation proves that there is not any major scratch or galling effect in the plates.

The finite element model (FEM) precisely predicted the hysteresis response of the RSFJ. The results demonstrated the existence of the bending moment in the cap plate. This bending moment could influence the design of the connection; therefore, it should be considered when designing an RSFJ. The distribution of the horizontal force between the grooves was shown to elaborate on the load transfer route in the connection. This could be employed in developing a simplified method for analysing RSFJs. The tension force of the bolts showed that all the bolts experience the same amount of tension when the RSFJ is in action. Since the RSFJ provides damage-free ductility, a higher ductility factor could be adopted when dissipative connections such as RSFJ are implemented in timber buildings. The use of RSFJ leads to a more economical design for structures with ductility of one.

Full-Scale Timber Column with RSFJ

In this study, tests on the LVL timber column having two RSFJs subjected to uniaxial (in-plane and out-of-plane) and biaxial loads were conducted. The RSF is presented in Figure 16. The two one-sided grooved cap plates and two two-sided grooved middle plates are bolted together in which the bolts are positioned in the middle of the slotted holes of the middle plates. The disc springs are also placed on the cap plates to provide room for the upward and downward movement of the cap plate when the horizontal force exceeds the friction force between the plates. The amount of friction force depends on the prestressing force of the bolts, the angle of the grooves, and the coefficient of friction between the plates. The spherical plain bearing is also added to have a fully pin behaviour in the out-of-plane direction. The specification of the employed bearing is given in the following sections.



Figure 16: RSFJ for column testing

The free body diagram of the symmetric RSFJ was used to determine the value of different points in the flag-shaped hysteresis curve such as the sliding force, the ultimate capacity, the restoring, and the residual forces to specify the behaviour of the joint theoretically. The sliding force of the joint can be determined from the equilibrium of forces acting on the slip friction plates. Furthermore, a very thin layer of grease is also applied to the friction surfaces during the assembly to ensure that the surfaces remain free of significant scratch over the design life of the structure and that the hysteresis curve is repeatable. Detailed discussion on the performance of the joint and its equations are provided in the previous chapters.

The connection of this test was evaluated through a finite element analysis using the software ABAQUS [25]. The RSFJ has a 1000 kN capacity and the sliding force is approximately 400 kN. A prestressing force of 60 kN has been applied to the 12 M20 bolts to have around 400 kN sliding force. The connection was designed to be able to expand under a tension force and to behave like a rigid member under the compression force, as there is no gap provided between the middle plates. Thus, the middle plates almost touch each other. As a result, the point of rotation in the column would be either of the joints during the cyclic loads for the uniaxial in-plane test, while the other joint would expand. Hence, the lever arm for calculating the axial force in the joints will be determined as the distance from the centre to centre of the RSFJs, which is 860 mm. The goal of these experiments was to corroborate the cyclic behaviour as well as the structural response of the system. Other parameters were also monitored such as the stiffness and the equivalent damping ratio of the column assembly and the RSFJs.

Due to the available laboratory facilities, the test set-up demonstrated in Figure 17 was designed and constructed. In addition to the specimen, the other equipment involved in the experiment includes a hydraulic actuator with the capacity of ± 330 kN and 250 mm stroke (used for the in-plane loading) and a hydraulic jack with the same capacity and a 150 mm stroke (used for applying the out-of-plane displacement). A data logger system is also hooked up to a computer to monitor the load and displacement recordings. The setup was assembled on the strong floor of the University of Auckland Test Hall. The end of the actuator and the hydraulic jack were fixed to the strong wall with four M40 anchors, and the other side of the actuator and the hydraulic jack were attached to the LVL column. The column was bolted to the base plate with two RSFJs. As shown in Figure 17, portal gauges were installed between the two middle plates

to measure the opening of the joint. LVDTs and a laser were placed to monitor the vertical movement of the end and the horizontal displacement of the column respectively. Another LVDT was also installed on the end bracket to measure any possible sliding that could influence the test result. Time histories of both displacement and force were recorded by the data acquisition system (DAQ) set up on a 0.1 Hz sampling rate.



Figure 17: Experimental setup for testing the column

Figure 17 shows a close-up of the instrumentation and the RSFJ. The out-of-plane deflection of the column was restricted by providing lateral support for the in-plane test. The supports were removed when the out-of-plane and the bi-directional tests were conducted. The test set-up showed a solid behaviour and no damage was observed after the tests were completed. Regarding the in-plane direction, the actuator was employed to implement the displacement, and concerning the out-of-plane direction, the hydraulic jack was used to apply the loading. With regards to the bi-directional testing, both actuator and jack were used simultaneously to load the column at 16 degrees (100:30 ratio), to comply with the code requirements. The specimen was loaded cyclically with the actuator. The cyclic loading protocol is in the format of inter-storey drift angle (θ). The protocol starts with four cycles at $\theta=0.005$ rad followed by four cycles at $\theta=0.01$ rad, and four cycles at $\theta=0.02$ rad in backward and forward directions. The loading protocol goes to maximum drift of 2% for the in-plane test. The out-of-plane test was performed in four different cycles. The first cycle was carried out with 0.5% drift, followed by 1%, 2%, and 3% drift in both forward and backward directions. The specimen was loaded cyclically through the actuator and the hydraulic jack. The protocol starts with four cycles at $\theta=0.01$ rad followed by four cycles at $\theta=0.02$ rad, and four cycles at $\theta=0.025$ rad. The loading protocol goes either to maximum drift of 2.5 % or the in-plane force of 300kN (whichever has less force). Therefore, the maximum applied load was governed by the minimum

of either of the 2.5% drift or the maximum capacity of the actuator, which is the same as the capacity of the shear key. Since the behaviour of the column is symmetric, the column was only pushed outwards in both out-of-plane and in-plane directions.

For clarity purpose, in the result discussion, the RSFJ refers to the casted plates, the connection refers to the entire assembly (including the pin brackets), and the column refers to the entire assembly. All column loading and displacement recordings are reported at the height of 2.6 m.

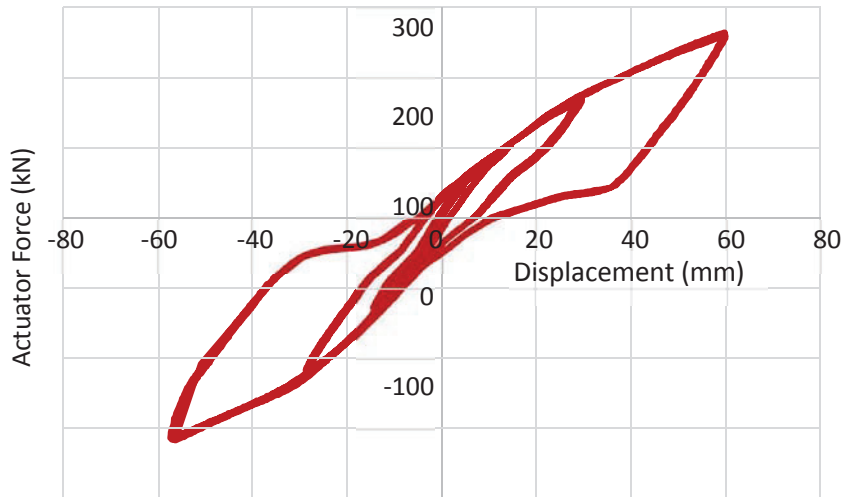


Figure 18: In-plane hysteresis curve of the column

The column load-displacement behaviour was measured, and the observations on the column and RSFJs assembly are made from the analysis of these different load-deformation curves. Upon loading of the column in the in-plane direction, elastic deformation of the system took place. Initially, the RSFJ did not open. After that, stiffness reduction started to appear when the RSFJ opened. The hysteresis curve shown in Figure 18 illustrates the cyclic performance of the column, and the one in Figure 19 is for the RSFJ itself (recording the middle plates relative displacements). Referring to the in-plane results (Figs. 18), the intersection of the hysteresis curve with the displacement axis could imply some residual drift, which in fact is misleading and brings one to conclude that the column is not self-centring. To demonstrate that such behaviour is related to the test set-up and not the tested structure, separate half cycle tests were conducted under the actuator in tension, the results are shown in Figures 19.

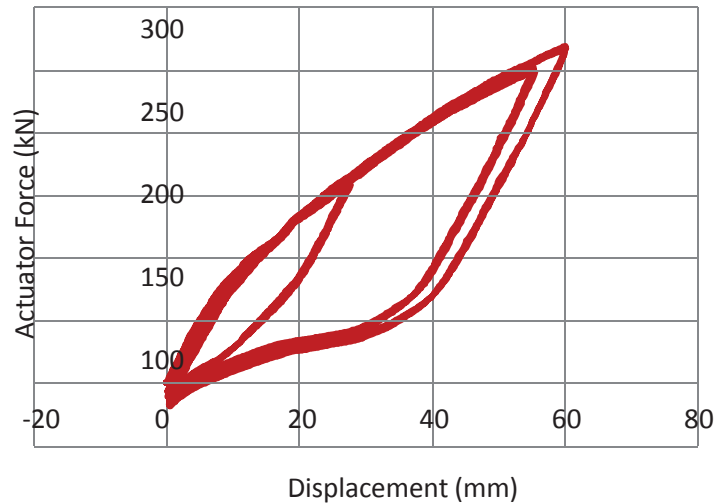


Figure 19: In-plane hysteresis curve of the column in the half cycle

The column is fully self-centring, whereas, in the full cycle, there is a small residual drift. This can be explained by some minor misalignment of the actuator under compression due to the test set-up having some freedom of rotation to some extent (potentially causing some column torsion) requiring extra force to overcome the effect of this misalignment during re-centring. This torsion effect would not occur in reality. It should be mentioned that an elastic deflection of 0.8 mm has been measured between the RSFJ top pin bracket and the column (due to the threaded rods elastic elongation). Also, a minor 0.3 mm uplift between the bottom bracket and the base has been recorded.

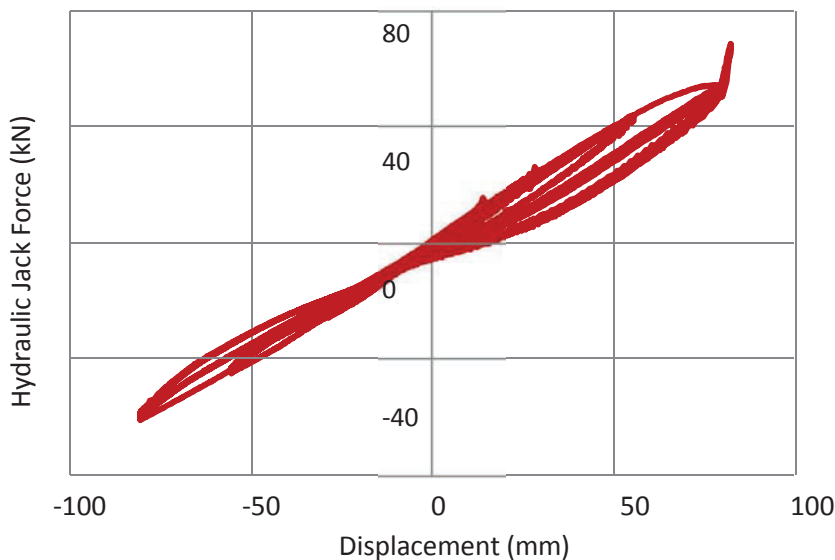


Figure 20: Out-of-plane hysteresis curve of the column

Although the application of the spherical bearing eliminates any bending moment in the connection, the column still has some resistance in the out-of-plane direction. The reason is the existence of the 150 mm eccentricity (half of the column width) between the centre of rotation (edge of the column bottom plate) and the connection axis. Figure 20 shows the load- deformation curve of the column.

The main results of the bi-directional test are summarized in Figures 21 and 22. The displacement reported in this paper was measured at the level of 2.6m. The test was performed to satisfy 30% of displacement in Y-direction and 100% of displacement in X-direction, which is equivalent to testing the column with 16 degrees of rotation. In this cyclic testing, the column was first moved in the out-of-plane direction followed by the corresponding displacement in the in-plane direction. To investigate the effect of the bi-axial loading on the performance of the RSFJ and the column, the shear force and the displacement were measured in both X and Y directions. During the test, no considerable torsion was observed in the assembly. Figures 21 and 22 indicate the actuator load versus displacement for the in-plane and out-of-plane directions. All of the connections and the column show an elastic response up to the 2.5% drift. The bidirectional results demonstrate a small rise in the stiffness of the overall system compared with the in-plane test results. As illustrated in Figure 21, the sliding in the RSFJs occurred at the actuator force level of 135 kN.

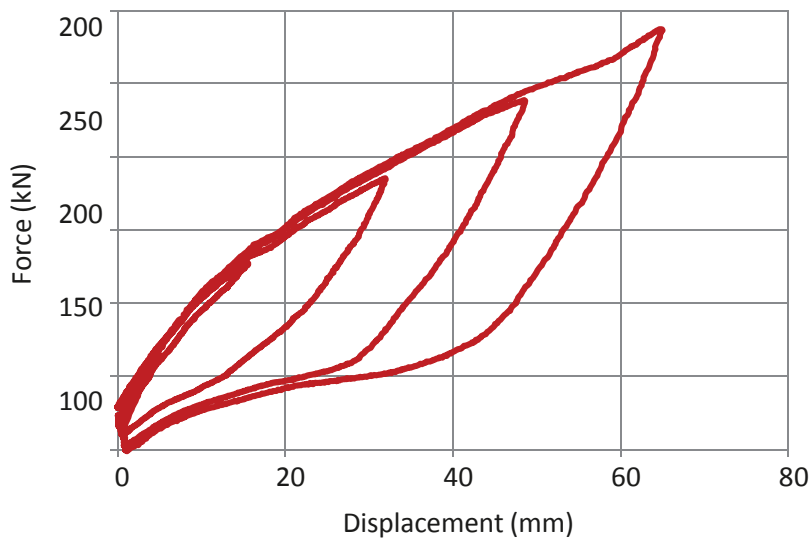


Figure 21: In-plane hysteresis curve of the column in the bi-directional test

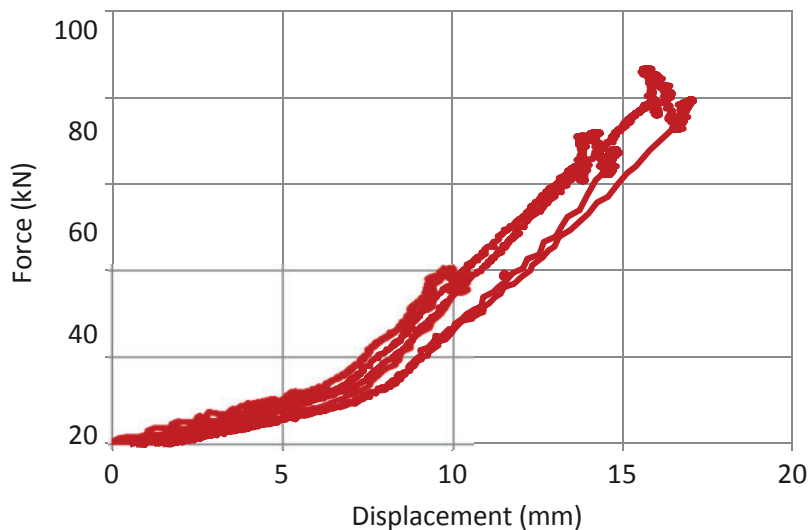


Figure 22: Out-of-plane hysteresis curve of the column in the bi-directional test

The lever arm is 2.6 m, and the eccentricity is 0.86 m measuring from centre-to-centre of the RSFJs at two sides of the column. Thus, the axial force of the RSFJ is equivalent to 408 kN. The RSFJ's opening and the displaced shape (out-of-plane) of the column are presented in Figure 22.

Hybrid Building with RSFJ

Hybrid construction effectively exploits the structural advantage of components with different materials. Since timber inherits a high strength to weight ratio, the timber elements are likely to be lighter than other element types. Therefore, earthquake forces which are related to the weight of the structure would be reduced in the structures using timber members. By combining steel and timber components, the benefits of each material could compensate some structural limitations of the other material.

This study investigates the ductility that the RSF joints can provide for the timber-steel hybrid structure. Furthermore, the dynamic response of the building equipped with the RSF joints is assessed. This connection can provide self-centring for the structure and add the energy dissipation mechanism to the building. There is a lack of self-centring in the conventional slip friction joints, although some studies have been carried out to add a self-centring feature to the connection [26].

A 10-storey hybrid building (timber beams-steel columns) with moment resisting frame system was considered for this study. It was considered that the building is located in Wellington, New Zealand, which is categorised as a high seismic zone, and a soil class C was chosen for the analysis based on the New Zealand Standard for Structural Design Actions [24]. Wellington has the highest hazard factor compared to other cities in New Zealand, and therefore, it can refer to the most critical scenario. The 3D view and the floor plan of the building are shown in Figure 23. The floor plan is 27 m by 27 m, and the structure has a floor height of four metres. The seismic masses for each floor were calculated using the New Zealand Standard for Structural Design Actions [24].

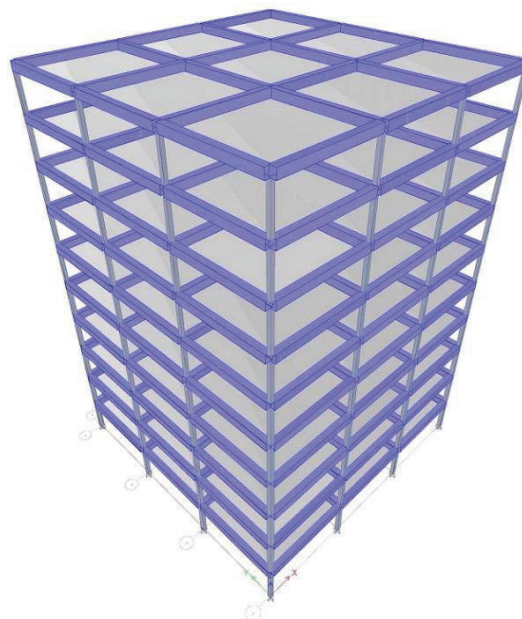


Figure 23: Structural configuration.

The bending moment demands of the connections were obtained through the equivalent static analysis regarding a structural ductility level (μ) of one. The building was designed with the goal of being ready for re-occupancy after experiencing the design basic earthquake.

The structure is modelled in 3D using SAP 2000 programme [23]. The equivalent static method was carried out to determine the section size of the beams and the columns. The ductility factor of one is considered for the building since the formation of hinges in timber beams is not permitted, and it is not preferable to have plastic hinges in the columns. Given that the centre columns are just carrying gravity loads, the outer frames and the columns withstand the lateral load. The structure has the fundamental period of 1.9s. The diaphragm has been considered rigid in the model.

A push-over analysis was conducted on the building designed with a ductility level of one and equipped with the RSF joints to obtain the modified displacement ductility factor for the building. The push-over analysis provides information regarding the response characteristics which can not be captured through other types of analyses. Based on the above expression the target displacement of 55 cm was obtained for the building. The result of the push-over analysis is shown in Figure 24 where the bilinear elasto-plastic behaviour of the building was drawn based on the equal energy method. In this approach, the area surrounded by the actual behaviour above the elasto-plastic approximation should be equal to the area enclosed by the real behaviour below the elasto-plastic approximation. Consequently, the displacement ductility ratio of two is calculated for the building.

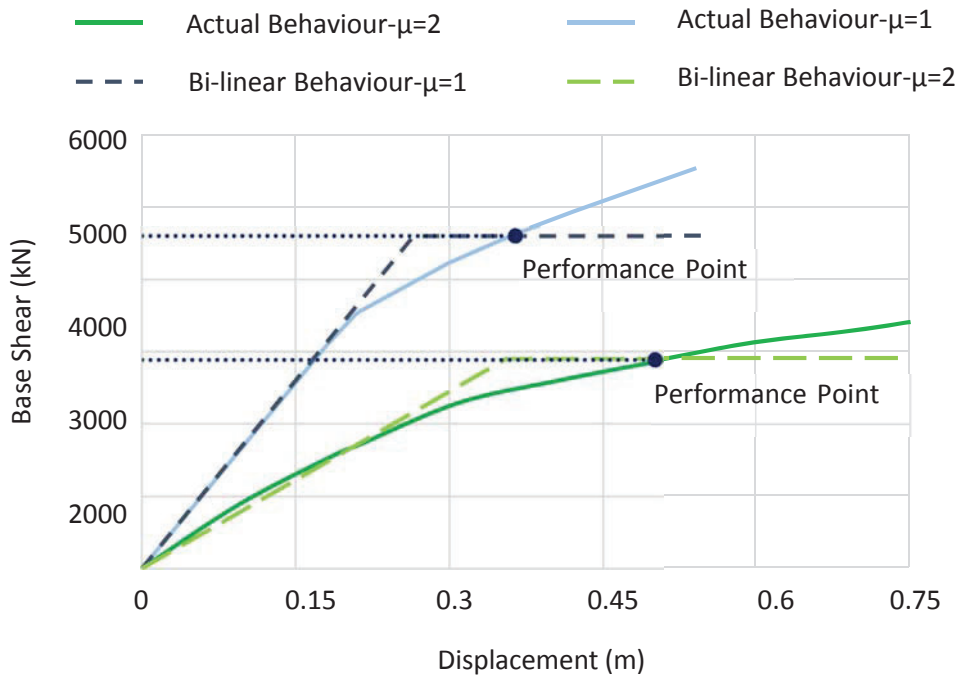


Figure 24: Push-over analysis result for two buildings with different ductility levels

The performance point can also be achieved by superimposing capacity spectrum and demand spectrum

where the intersection point of these two curves specifies performance point [27]. The performance point of the building is specified in Figure 24. The performance displacement of the structure is 36 cm with the base shear of 4593kN.

A new building was designed using the obtained ductility of two, and the members' section sizes are optimised as indicated in Table 1. In this section, the correctness of the calculated ductility will be checked.

Table 1: Members and materials properties for a building with ductility level of 2

	Outer Frame		Inner Frame	
Story	Column (mm)	Beam (mm)	Column (mm)	Beam (mm)
1-6	Box 400x400x25	800x600	Box 400x400x25	610x450
7-10	Box 350x350x20	800x600	Box 350x350x20	610x450
Material properties				
Column	Hot-rolled Steel			
Beam	LVL 11			

Members' section sizes were decreased since the building was designed with the ductility of two but this reduction in the size of beams section could have been more since the demand was considerably reduced. However, this was not achievable since the drift was exceeding the limitation of 2.5%. The newly designed structure has the fundamental period of 2.1s. The push-over analysis was repeated for the new structure to check the correctness of the ductility. The result of the analysis is presented in Figure 24 in which the graph corroborates the accuracy of the calculated ductility value of 2.

The maximum values of displacement when the RSFJs were used are given in Table 2. It is shown that the maximum top floor displacement was increased due to the existence of the RSF joints while this value is still satisfying the allowable displacement criteria. Therefore, by installing RSF joints in the system, the buildings are allowed to have more horizontal deflection while the horizontal deflection should still be in the acceptable range.

Table 2: Top floor displacement

Record	Displacement without RSFJ ($\mu=1$) (m)	Displacement with RSFJ ($\mu=1$) (m)	Increase (%)	Displacement without RSFJ ($\mu=2$) (m)	Displacement with RSFJ ($\mu=2$) (m)	Increase (%)
El Centro	0.27	0.31	15.3	0.35	0.46	29.6
Hokkaido	0.3	0.32	7.6	0.31	0.32	4.2
Tabas	0.3	0.33	11.2	0.35	0.39	13.4

The maximum values of acceleration when RFS joints were used are given in Table 3. It is shown that the maximum base shear decreases effectively. The reduction is varying from 11.3% to 30.1% and from 35% to 39.9% for different ground motions regarding the structures with ductility of one and two respectively.

Table 3: Top floor acceleration

Record	Acceleration without RSFJ ($\mu=1$) (m/s ²)	Acceleration with RSFJ ($\mu=1$) (m/s ²)	Reduction (%)	Acceleration without RSFJ ($\mu=2$) (m/s ²)	Acceleration with RSFJ ($\mu=2$) (m/s ²)	Reduction (%)
El Centro	4.19	2.93	30.1	4.99	3	39.9
Hokkaido	4.32	3.59	16.9	4.4	2.8	35.2
Tabas	5.5	4.88	11.3	5.88	3.82	35

Conclusions

The main research conclusions can be summarised as below:

- a. For the optimum performance of the structure equipped with RSFJ, in terms of the base shear and the maximum drift, the sliding threshold in the range of 50% to 75% of the connected members under the design basic earthquake is recommended.
- b. The repeatability of the hysteresis curve is directly under the influence of the surface roughness of the RSFJ plates and the lubrication that is used for the contact surfaces.
- c. The RSFJ could add a self-centring characteristic to the structure while providing some portion of energy dissipation as well.
- d. The bolts in the RSFJ are in pure tension, and they are unlikely to need replacing after a strong ground motion.
- e. The disc springs showed elastic behaviour under more than 100 cycles and demonstrated a consistent performance.
- f. The load distribution between the RSFJ grooves is not even, and it should be considered when designing the connection.
- g. Because of load eccentricity when the RSFJ is open, there would be an additional bending moment in the cap plate, which should be encountered for the RSFJ design.
- h. The application of RSFJs in structures, specifically in the structures with the ductility factor of one could lead to a higher ductility factor.

Future work

This research has demonstrated the rocking performance of the beam column connection equipped with two RSFJs and developed basic guidelines for designing the RSFJ. The following recommendations would further develop the knowledge database. There are still questions remaining on different aspects of having RSFJs in structures. Some potential topics are summarised here for future study possibilities.

- a. Develop a displacement-based design graphs to provide the damping ratio and the ductility factor for different structural systems to be used in the design process.*
- b. Friction dampers are usually get adopted for mid-rise building, so it is recommended to evaluate the effectiveness of the RSFJ for both low-rise and high-rise buildings to find out about the damping ratio in these types of structures.*
- c. The inherent characteristic of the flag shape hysteresis curve is the energy dissipation ability in only two quadrants of the load-displacement curve. This feature makes the energy dissipation of the system less in comparison with the systems that act in all the quadrants. Therefore, a suitable range of structures should be presented that can take the most out of the RSFJs application.*
- d. The influence of having RSFJs in the buildings should be studied on the non-structural elements by assessing the acceleration response since for the structural performance the focus is on the horizontal deflection.*
- e. Further study can be dedicated to studying the performance of the RSFJ after the ultimate load and providing a secondary fuse in the system.*
- f. The rotation of the connection and the prying effect could be another area of interest as in many applications; the RSFJ would be under rotation.*
- g. Different buildings with different periods should be investigated using wide range of records including near-field and far-field ground motions to have an in-depth understanding of the RSFJs effect on different structures.*
- h. Finally, a shake table test is recommended on a scaled structure using the obtained knowledge to design the structure and to assess a structure under dynamic tests.*

Acknowledgements

This study has been financially supported by the New Zealand Earthquake Commission (EQC) and Uniservices at the University of Auckland. Financial support from these institutions is greatly appreciated.

References

- [1] M. J. N. Priestley, S. Sritharan, J. R. Conley and S. Pampanin, "Preliminary Results and Conclusions from the PRESSS Five-Story Precast Concrete Test Building," PCI Journal, Vol. 44(6), 42-67, 1999.*
- [2] Y. C. Kurama, S. Pessiki, R. Sause and L. W. Lu, "Seismic Behavior and Design of Unbonded Post-Tensioned*

Precast Concrete Wall," *PCI Journal*, Vol. 44(3), 72-89, 1999.

[3] J. M. Ricles, R. Sause, S. W. Peng and L. W. Lu, "Experimental Evaluation of Earthquake Resistant Post-tensioned Steel Connections," *Journal of Structural Engineering*, Vol. 128(7), 850-859, 2002.

[4] J. M. Ricles, M. Sause, M. Garlock and C. Zhao, "Post-Tensioned Seismic Resistant Connections for Steel Frames," *Journal of Structural Engineering*, Vol. 127(2), 113-121, 2001.

[5] M. Garlock, J. M. Ricles and R. Sause, "Experimental studies on Full-Scale Post Tensioned Steel Connections", *Journal of Structural Engineering*, Vol. 131(3), 438-448, 2005.

[6] P. Rojas, J. M. Ricles and R. Sause, "Seismic Performance of Post-Tensioned Steel Moment Resisting Frames with Friction Devices", *Journal of Structural Engineering*, Vol. 131(4), 529- 540, 2005.

[7] D. Roke, R. Sause, J. M. Ricles, C. Y. Seo and K. S. Lee, "Self-Centering Seismic- Resistant Steel Concentrically-Braced Frames," in *8th U.S. National Conference on Earthquake Engineering, San Francisco, 2006*.

[8] M. R. Eatherton, J. Hajjar, H. Krawinkler and G. Deierlein, "Seismic Design and Behavior of Steel Frames with Controlled Rocking – Part I: Concepts and Quasi-Static Subassembly Testing," *ASCE/SEI Structures Congress, 2010*.

[9] D. Roke, R. Sause, J. M. Ricles and N. B. Chancellor, "Damage-Free Seismic Resistant Self-Centering Concentrically-Braced Frames," *Lehigh University, Bethlehem, 2010*.

[10] M. Danner and C. Clifton, "Development of Moment-Resisting Steel Frames Incorporating Semi-Rigid Elastic Joints," *Heavy Engineering Research Association, Manukau, 1995*.

[11] N. Priestley and G. A. MacRae, "Seismic Tests of Precast Beam-to-Column Joint Subassemblages with Unbonded Tendons," *PCI Journal*, Vol. 41(1), 64-80, 1996.

[12] C. Clifton, "Semi-rigid joints for moment-resisting steel framed seismic-resisting systems," *Department of Civil and Environmental Engineering, University of Auckland, Auckland, 2005*.

[13] M. Garlock and J. Li, "Steel Self-Centering Moment Frames with Collector Beam Floor Diaphragms," *Journal of Constructional Steel Research*, Vol. 64(5), 526-538, 2008.

[14] A. King, "Design of Collector Elements for Self-Centering Moment Resisting Frames," *Master of Science in Civil Engineering, Purdue University, 2007*.

[15] C. C. Chou and J. H. Chen, "Development of Floor Slab for Steel Post-Tensioned Self- Centering Moment Frames," *Journal of Constructional Steel Research*, Vol. 67(10), 1621- 1635, 2011.

[16] M. Mohammad, E. Gagnon, E. Karacabeyli and M. Popovski, "Innovative Mid-rise Timber Structures Offer New Opportunities for Designers," *Structural Engineers Association of California, Las Vegas, 2003*.

[17] A. Filiatrault and S. Cherry, "Performance Evaluation of Friction Damped Braced Steel Frames under Simulated Earthquake Loads," *Journal of Earthquake Spectra*, Vol. 3(1), 57-78, 1987.

[18] C. E. Grigorian and E. P. Popov, "Energy Dissipation with Slotted Bolted Connections," *Earthquake Engineering Research Centre, Berkeley, 1994*.

[19] C. E. Grigorian, T. S. Yang and E. P. Popov, "Slotted Bolted Connection Energy Dissipators", *Journal of Earthquake Spectra*, Vol. 9(3), 491-504, 1993.

[20] T. S. Yang and E. P. Popov, "Experimental and Analytical Studies of Steel Connections and Energy Dissipators", *Earthquake Engineering Research Center, Berkeley, 1995*.

[21] G. MacRae, C. Clifton, H. Mackinven, N. Mago, J. Butterworth and S. Pampanin, "The Sliding Hinge Joint Moment Connection", *New Zealand Society of Earthquake Engineering Conference, 2010*.

[22] NZS 3404, "Steel structures standard", *Standards New Zealand. Wellington, New Zealand, 2009*.

[23] CSI, *SAP2000 Integrated Software for Structural Analysis and Design*, *Computers and Structures Inc., Berkeley, California*.

[24] NZS 1170.5, "Structural Design Actions", Standards New Zealand, 2004.

[25] ABAQUS Analysis user's manual version 6.14. ABAQUS Inc.; 2014.

[26] H. Khoo, C. Clifton, J. Butterworth and G. MacRae, "Development of the self-centering sliding hinge joint with friction ring springs", *Journal of Constructional Steel Research*, Vol. 78, 201-211, 2012.

[27] ATC-40, "Seismic evaluation and retrofit of concrete buildings: Volume 1". Applied Technology Council, Report No. SSC 96-01, 1996.

Outputs

Valadbeigi A., Zarnani P., and Quenneville P.: *Determining the optimum slip load of the friction damped concentrically braced multi-storey timber frame. Proceedings of the 10th Pacific Conference: Earthquake Engineering Building an Earthquake-Resilient Pacific, 2015. Sydney, Australia.*

Valadbeigi A., Zarnani P., and Quenneville P.: *Dynamic evaluation of hybrid timber-steel moment frame structure using Resilient Slip Friction connections. WCTE 2016: World Conference on Timber Engineering, 2016. Vienna, Austria.*

Valadbeigi A.: *Application of a resilient slip friction connection in hybrid timber-steel structures. Provisional Seminar Report, University of Auckland, 2016. Auckland, New Zealand.*

Zarnani P., Valadbeigi A., and Quenneville P.: *Resilient slip friction (RSF) joint: A novel connection system for seismic damage avoidance design. WCTE 2016: World Conference on Timber Engineering, 2016. Vienna, Austria.*

Hashemi A., Zarnani P., Valadbeigi A., Masoudnia P., and Quenneville P.: *Seismic resistant cross laminated timber structures using innovative resilient friction damping system. NZSEE 2016: The New Zealand Society for Earthquake Engineering, 2016. Christchurch, New Zealand.*

Hashemi A., Zarnani P., Valadbeigi A., Masoudnia P., and Quenneville P.: *Seismic resistant timber walls with new Resilient Slip Friction damping devices. INTER 2016: International Network on Timber Engineering Research, 2016. Graz, Austria.*

Valadbeigi A., Zarnani P. and Quenneville P.: *Bi-directional experimental behaviour of a timber column with resilient slip friction joint. NZSEE 2018: The New Zealand Society for Earthquake Engineering, 2018. Auckland, New Zealand.*

Valadbeigi A., Zarnani P., and Quenneville P.: *Cyclic Performance of a Full-scale Timber Column Equipped with Resilient Slip Friction Joints. INTER 2018: International Network on Timber Engineering Research, 2018. Tallinn, Estonia.*

Links to publications/theses

Valadbeigi A.: *Application of a Resilient Slip Friction Joint in Steel-Timber Hybrid Structures. PhD thesis submitted in partial fulfillment for the degree of Doctor of Philosophy of the University of Auckland, 2019. Auckland, New Zealand.*

List of key end users

Design consultants